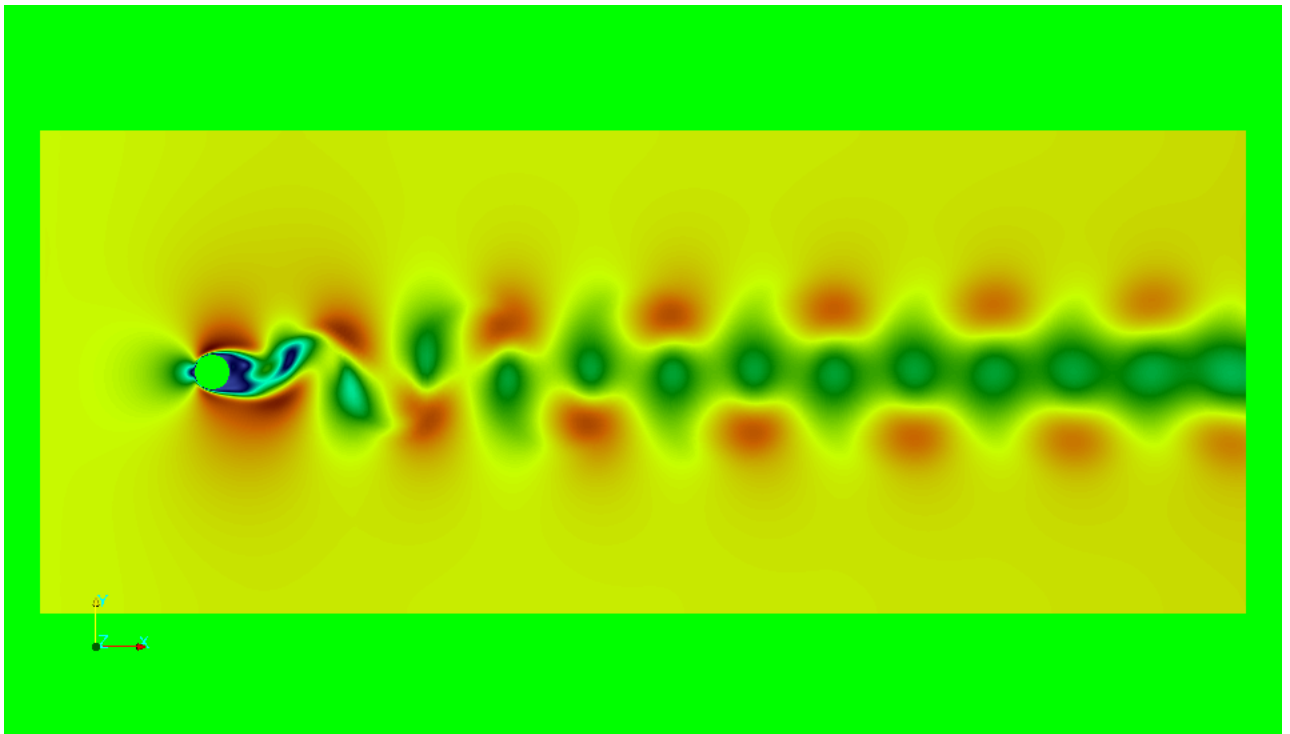


# CFD SIMULATIONS OF LAMINAR VORTEX SHEDDING WITH OPENFOAM

---

MARTIN EINARSVE, MSc



## Preface

This review is meant to be an introduction to the open source CFD package openFoam developed by OpenCFD, distributed by the OpenFOAM Foundation and licensed under GNU General Public License <sup>1</sup>. It is hoped that this tutorial will contribute to the openFoam learning community and perhaps ease the introduction to openFoam, as it is fair to say that it is a bit difficult getting started with openFoam.

In this report we also consider relevant fluid dynamical theory, meshing and post processing. The full case folder is to be found and downloaded at

<https://github.com/meinarsve/CFDwOpenFoam/tree/master/LaminarVortexSheddingInOpenFoam> which contains the openFoam files, mesh file, and post processing scripts to plot relevant data in Matlab, and an R-script to clean the output files from openFoam. Additional video tutorials on case setup may be found at

<https://www.youtube.com/watch?v=aIvDtyAYnI8>. In general the learner may find many useful video tutorials on Youtube. It should be stated that this document in no way is to be taken as official openFoam teaching material.

Martin Einarsve, Nov 2015

---

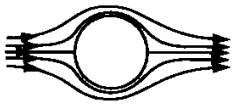



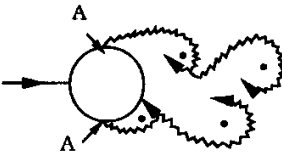

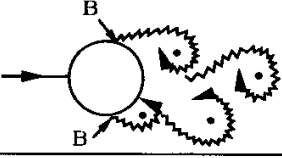
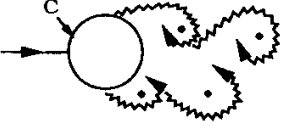
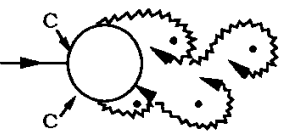
<sup>1</sup><http://www.openfoam.com/>

## CFD simulations of Laminar Vortex Shedding with openFoam

In this review we are going to work through and try to understand the flow regimes produced by a cylinder in crossflow and in particular the phenomenon of Vortex Shedding, one of many fun, interesting and non-linear phenomena of fluid dynamics. We will attack the problem using the open source CFD solver openFoam, and thus this document will work as a tutorial and introduction to many features of openFoam. Along the line we will discuss relevant fluid dynamical theory as well, including dimensional analysis, drag/lift forces on the cylinder and Fourier frequency analysis of time signals. Vortex Shedding occurs when an object such as a cylinder or sphere is subjected to a free stream cross flow which will result in vortices being shed in the wake of the cylinder, also known as a von Karman Vortex Street. The problem of cylinder subjected to cross flow is important in many engineering disciplines, say heat transfer applications in heat exchangers, and pipelines/risers in offshore engineering to name a few. It is also a very well suited starting point to gain acquaintance with CFD simulations for many reasons. Firstly the problem lends itself to 2D simulations, which is a must to any person who want to perform CFD calculations on his/her personal computer. As most CFD simulations are considerably time consuming to run, it is necessary to be quite familiar with all aspects of 2D CFD simulations before one attempts to perform 3D simulations. This tutorial is also designed to be suitable for ordinary laptop computers, with  $\leq 8$  GB RAM with CFD simulation lengths ideally no longer than a few hours, so this puts considerable limits on the number of cells in the computational domain. We therefore stick to 2D simulations, as it is better to have a considerable resolved 2D flow field, than a poorly resolved 3D flow field.

Secondly the geometry is sufficiently complex, such that we need to pay deliberate attention to the meshing, thus it is a great starting point to learn how to produce an acceptable mesh for the problem. As meshing is absolutely crucial to produce reasonable CFD results, this will introduce the do's and dont's on how to produce good meshes, and how to distinguish good meshes from poor ones.

Thirdly it is external flow, which introduces the peculiarities of the farfield boundary conditions. If we had chosen an internal flow i.e. pipeflow as an example we would only have been exposed to the no-slip boundary conditions on the walls, besides the inlet/outlet bc.

a) 	No separation. Creeping flow	$Re < 5$
b) 	A fixed pair of symmetric vortices	$5 < Re < 40$
c) 	Laminar vortex street	$40 < Re < 200$
d) 	Transition to turbulence in the wake	$200 < Re < 300$
e) 	Wake completely turbulent. A: Laminar boundary layer separation	$300 < Re < 3 \times 10^5$  Subcritical
f) 	A: Laminar boundary layer separation B: Turbulent boundary layer separation; but boundary layer laminar	$3 \times 10^5 < Re < 3.5 \times 10^5$ Critical (Lower transition)
g) 	B: Turbulent boundary layer separation; the boundary layer partly laminar partly turbulent	$3.5 \times 10^5 < Re < 1.5 \times 10^6$  Supercritical
h) 	C: Boundary layer com- pletely turbulent at one side	$1.5 \times 10^6 < Re < 4 \times 10^6$ Upper transition
i) 	C: Boundary layer comple- tely turbulent at two sides	$4 \times 10^6 < Re$ Transcritical

**Figure 1:** Flow regimes of flow around a circular cylinder. From [Sumer et al]. Note that we will focus on the interval  $50 < Re < 300$  in this review.

# Laminar Vortex Shedding

A common problem of vast engineering importance in civil engineering is to analyse and understand the frequencies of the lift and drag forces on the cylinder induced by the shedding vortices. It is crucial that these frequencies do not coincide with the natural frequencies of the cylinder construction itself, or else the construction will hit resonance, and start to vibrate with unacceptable large amplitudes. Therefore frequency analysis is today widely documented for different geometries, and is something that engineers must pay special attention to.

## Dimensional Analysis

A well suited starting point to analyse this is to use the technique of dimensional analysis to gain a broad picture overview of the problem. Lets imagine a  $2D$  flow with characteristic free stream velocity  $U$  across a cylinder of diameter  $D$ , with fluid properties  $\rho$  and  $\mu$ . Lets now say that we know that when the cylinder is subjected to this type of cross flow, vortices will be shed in the wake of the cylinder, and we want to investigate the frequency of the vortex shedding  $f$ . In other words we want to investigate the functional relationship

$$f = func(U, D, \rho, \mu) \quad (1)$$

where  $f$  is in units  $[1/s]$ . The Buckingham Pi theorem says that any functional relationship with a total of  $n$  variables including both the *dependent* and *independent* variables and physical constant (in our this  $n = 5$ ), can be reduced to a problem containing  $p = n - m$  non dimensional variables, where  $m$  is the total number of dimensions of the dimensional problem. The process of doing this is called the Method of Repeating Variables, and let us now use this method to reduce the above dimensional problem to an easier non dimensional problem.

In problem (1) the dimensions of the problem is mass  $[kg]$ , length  $[m]$ , and time  $[s]$ , so  $m = 3$ . Thus problem (1) can therefore be reduced to a problem with  $p = 5 - 3 = 2$  non dimensional variables of the form

$$\Pi_1 = func(\Pi_2)$$

where  $\Pi_1$  and  $\Pi_2$  are non dimensional groups.

We now need to pick  $p = n - m = 5 - 3 = 2$  repeating variables among the  $n = 5$  variables of the dimensional problem. The process of selecting these repeated variables takes some experience, but there are some guiding principles. The choice we make when we select which repeating variables to use, will dictate how the non dimensional variables  $\Pi_1$ , and  $\Pi_2$  will look like, so its a (very!) good idea that these non dimensional variables are easily recognizable nondimensionalized groups such as the Reynolds number. So even if we have some freedom in selection the repeated variables, there are some guiding principles we should follow. The first repeating variable should always be the depended variable of the problem, so we select the frequency  $f$  as the first repeated variable. If  $\mu$  is among the independent variables, it is almost always a good idea to choose  $1/\mu$  as the second repeated variable, as this usually reveals the Reynolds number, which is practically always important in any fluid dynamical problem. You will realize this by

doing alot of problems on dimensional analysis in fluid dynamics. So now we have selected  $[f, 1/\mu]$  as the repeating variables of the problem.

Now for *each* of the repeating variables, we are going to multiply the *selected* repeating variable, with the *other* variables in the problem raised to a power  $(U^a, r^b, \rho^c)$ , that ensures that the product becomes nondimensional. In other words we need to solve for the exponents  $[a, b, c]$  such that the product becomes non dimensional. In the following we will use square brackets  $[ ]$  to denote units, such that for example  $[m] = [meter]$ . The process goes as follows:

$$\Pi_1 = f \cdot U^a \cdot D^b \cdot \rho^c$$

$$[-] = \left[ \frac{1}{s} \right] \cdot \left[ \frac{m}{s} \right]^a \cdot [m]^b \cdot \left[ \frac{kg}{m^3} \right]^c$$

In order for the product at the right side to be non dimensional we require

$$s^{-1} \cdot s^{-a} = s^0 \rightarrow a = -1$$

$$kg^c = kg^0 \rightarrow c = 0$$

$$m^a \cdot m^b \cdot m^{-3c} = m^0 \rightarrow a + b - 3c = 0 \rightarrow b = 1$$

Now that we solved for  $a, b, c$  we find that our first nondimensional group is  $\Pi_1 = \frac{fD}{U} = St$  known as the Strouhal number. Since this non dimensional group arose from selecting  $f$  (the dependent variable) as the repeating variable,  $\Pi_1$  will be the dependent variable in the non dimensional problem.

Now we do the same thing for the second selected repeated variable namely  $1/\mu$ .

$$\Pi_2 = \frac{1}{\mu} \cdot U^a \cdot D^b \cdot \rho^c$$

$$[-] = \left[ \frac{ms}{kg} \right] \cdot \left[ \frac{m}{s} \right]^a \cdot [m]^b \cdot \left[ \frac{kg}{m^3} \right]^c$$

In order for the product at the right side to be non dimensional we require

$$s^1 \cdot s^{-a} = s^0 \rightarrow a = 1$$

$$kg^{-1} \cdot kg^c = kg^0 \rightarrow c = 1$$

$$m^1 \cdot m^a \cdot m^b \cdot m^{-3c} = m^0 \rightarrow 1 + a + b - 3c = 0 \rightarrow b = 1$$

So again when we have solved for  $a, b, c$  we see that the second non dimensional group is  $\Pi_2 = \frac{UD\rho}{\mu} = Re$ , the Reynolds number.

So the original dimensional problem of (1) has thus been reduced to a non dimensional problem

$$St = func(Re) \tag{2}$$

To determine this functional relationship we will resort to Computational Fluid Dynamics, and the rest of this review will focus on this.

## Lift and Drag Forces in the range $50 < \text{Re} < 300$

Arguably the most important thing to analyse when doing an external flow problem, is the induced lift and drag forces the fluid exerts on an object. The Drag is the component of the induced force that act in the x-direction parallel to the ground, and the Lift is the component of the induced force that act perpendicular the Drag. In other words, Drag and Lift are just fancy words for the  $x$  and  $y$  component of the induced force.

It is important to understand that the Drag/Lift force is due to two effects: the sum of the *pressure force* around the cylinder, and the sum of *viscous shear force*, also called skin friction around the cylinder. The pressure drag is defined as

$$D_{\text{Pressure}} = \int_S P_w \cdot \vec{n} dS \quad (3)$$

where  $\vec{n}$  is the normal vector to surface element  $dS$ , and  $P_w$  is the pressure on the cylinder wall at the point  $dS$ . This is intuitive to understand as the magnitude of pressure acting on the front half of the cylinder minus the magnitude of pressure acting on the rear part of the cylinder. We also know this by experience that if you ride a bike, you will feel a large pressure drag acting on the front of your body, whereas if you ride your bike behind a vehicle you won't feel near as much drag, because the pressure at the back of the vehicle is smaller than the pressure in front of it.

The skin friction drag is similarly defined as

$$D_{\text{viscous}} = \int_S \tau_w \cdot \vec{t} dS \quad (4)$$

where  $\tau_w$  is the wall shear stress at the cylinder wall at point  $dS$ , and  $\vec{t}$  is the tangential vector to the cylinder wall at point  $dS$ . For Newtonian fluids,  $\tau_w$  is proportional to the fluid viscosity  $\mu$  and the velocity gradient at the wall. Since laminar boundary layers have smaller velocity gradient at the wall than turbulent boundary layers, the overall skin friction drag is larger for turbulent boundary layer, than laminar ones.

For blunt objects such as a cylinder, the Pressure drag is by far the effect that contributes the most to the overall drag. Viscous drag is most important for highly streamlined bodies such as an air plane wing. Thus classical methods for reducing drag force of objects (streamlining) mainly consists of reducing the overall pressure drag, without paying too much attention to viscous drag. A good example of this is the roughened surface of a golf ball, which reduces the pressure drag, by inducing a turbulent boundary layer over the ball. A turbulent boundary layer has more inertia, and will follow the curvature of the ball longer than laminar boundary layer, therefore flow separation occurs later if the flow is turbulent. This greatly reduces the overall pressure drag, even though the surface drag is slightly larger for the roughened surface. It should be mentioned that for highly optimized streamlined objects such as a race car or an air plane wing,

a lot of research is going into active control of the boundary layer, to try to delay transition to turbulence in the boundary layer as long as possible, and thereby reducing the overall skin friction drag.

Equations (3) and (4) only makes sense if we were to know a mathematical solution to the flowfield over the cylinder. These kind of solutions are known in the case of creeping flow valid for  $Re \leq 1$  and for potential flow valid for irrationally flowfields. But in our case where we know a discrete numerical solution, equations (3) and (4) is utilized by multiplying the flow variables ( $P, \tau_w$ ) at the cells adjacent to the cylinder walls, by the surface area of that cell adjacent to the cylinder wall, and summing up all these patches across the cylinder surface.

It is also customary to work with a nondimensional form of the drag/lift forces known as the drag/lift coefficients

$$C_D = \frac{F_D}{\frac{1}{2}\rho A_{pro} U_\infty^2}, \quad C_L = \frac{F_L}{\frac{1}{2}\rho A_{pro} U_\infty^2} \quad (5)$$

where  $A_{pro}$  is the projected area in the streamwise direction, and  $U_\infty$  is then freestream velocity. By this definition we can obtain unique drag/lift coefficients for different geometries, and plot them as functions of  $Re$ . For a 3D flow field, the projected area of a cylinder is given as  $A_{pro} = Db$  where  $D$  is the diameter and  $b$  is the length in the lateral direction.

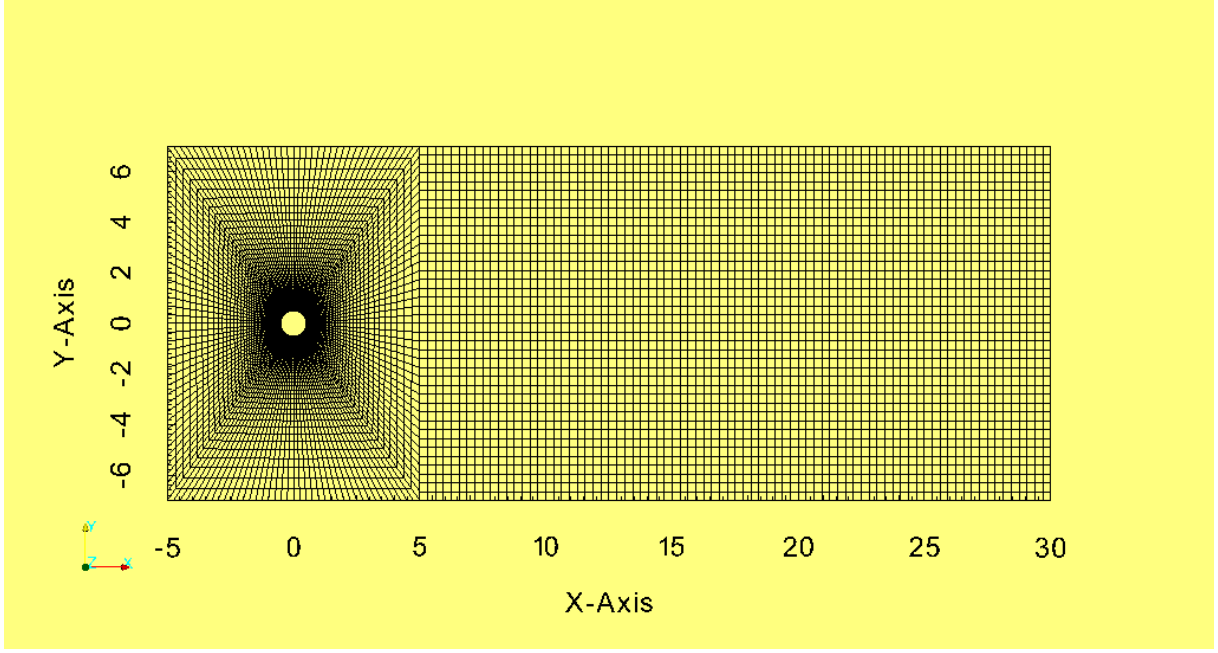
We have in the following performed a total of 6 simulations of Reynold numbers

$Re = [50, 100, 150, 200, 250, 300]$  as this is the range for laminar vortex shedding. All simulations are performed by *icoFoam* which is a Newtonian laminar transient solver which uses the PISO algorithm. Thus we are neglecting the fact that the wake becomes turbulent in the range  $200 < Re < 300$  as turbulent modelling is not the aim for this review. All simulations are performed over a timespan  $t = [0, 200]s$  with a cylinder diameter of  $D_{cyl} = 1m$  and an external geometry spanning  $x = [-5, 30]$ ,  $y = [-5, 5]$ , with the cylinder located at the origin, as seen in figure 2.

## Meshing

Producing a good mesh is necessary to produce reasonable solution. The mesh may influence the rate (or lack) of convergence, accuracy and CPU time. We have created a mesh consisting of 5 blocks with mesh mesh refinement near the cylinder wall to more accurately capture velocity gradients near the wall, as seen in figure 2. The mesh is created in the free software *gmsh* see <http://geuz.org/gmsh/>, and imported into openFoam with the command *gmshToFoam meshName.msh*.





**Figure 2:** Mesh of domain of simulation of a 2D cylinder, with mesh refinement around the cylinder.

In openFoam you may check the quality of the mesh with the utility `textitcheckMesh`. This utility checks that the mesh satisfies a minimum quality criteria, and if so will conclude with *Mesh Ok*. If `checkMesh` does not conclude with *Mesh Ok* you have to go back and improve your mesh. `checkMesh` also prints useful mesh data in the terminal and a description to this output may be found at <https://openfoamwiki.net/index.php/CheckMesh>. You should pay attention to:

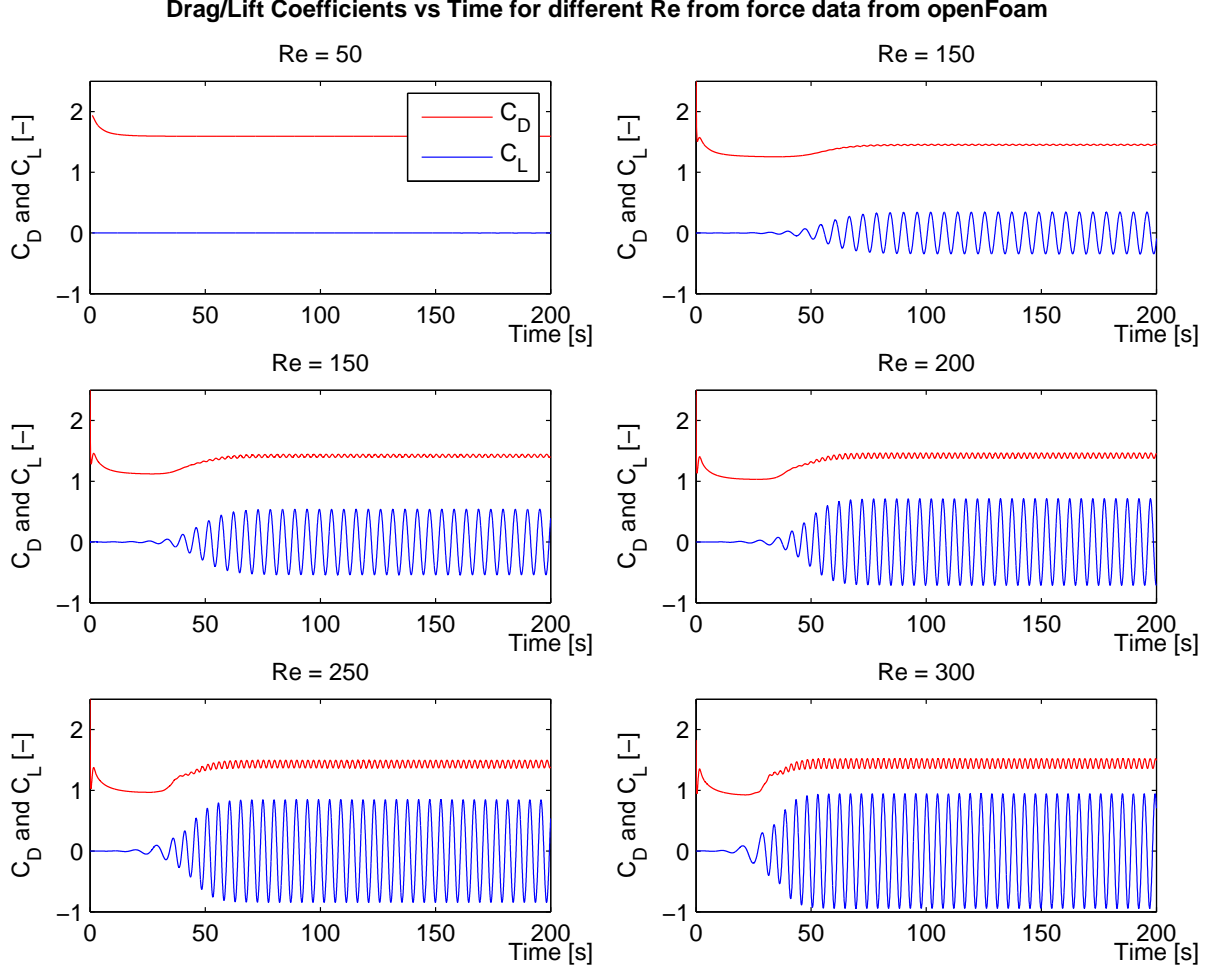
- *Max aspect ratio:* The ratio  $\frac{\text{max cell length}}{\text{min cell length}}$  of a cell. A value of 1.0 is best and try not to exceed a value of 100 – 1000.
- *max non orthogonality:* The smaller the better. If  $> 80^\circ$  running is difficult to achieve.
- *max skewness* The smaller value the better. This is a measure if how *pointy* the angles in the cells are. Ideally the angles in the cells should be as least pointy as possible. There are a few measures to measure skewness, one is

$$\frac{\text{optimal cellsize} - \text{actual cellsize}}{\text{optimal cellsize}}$$

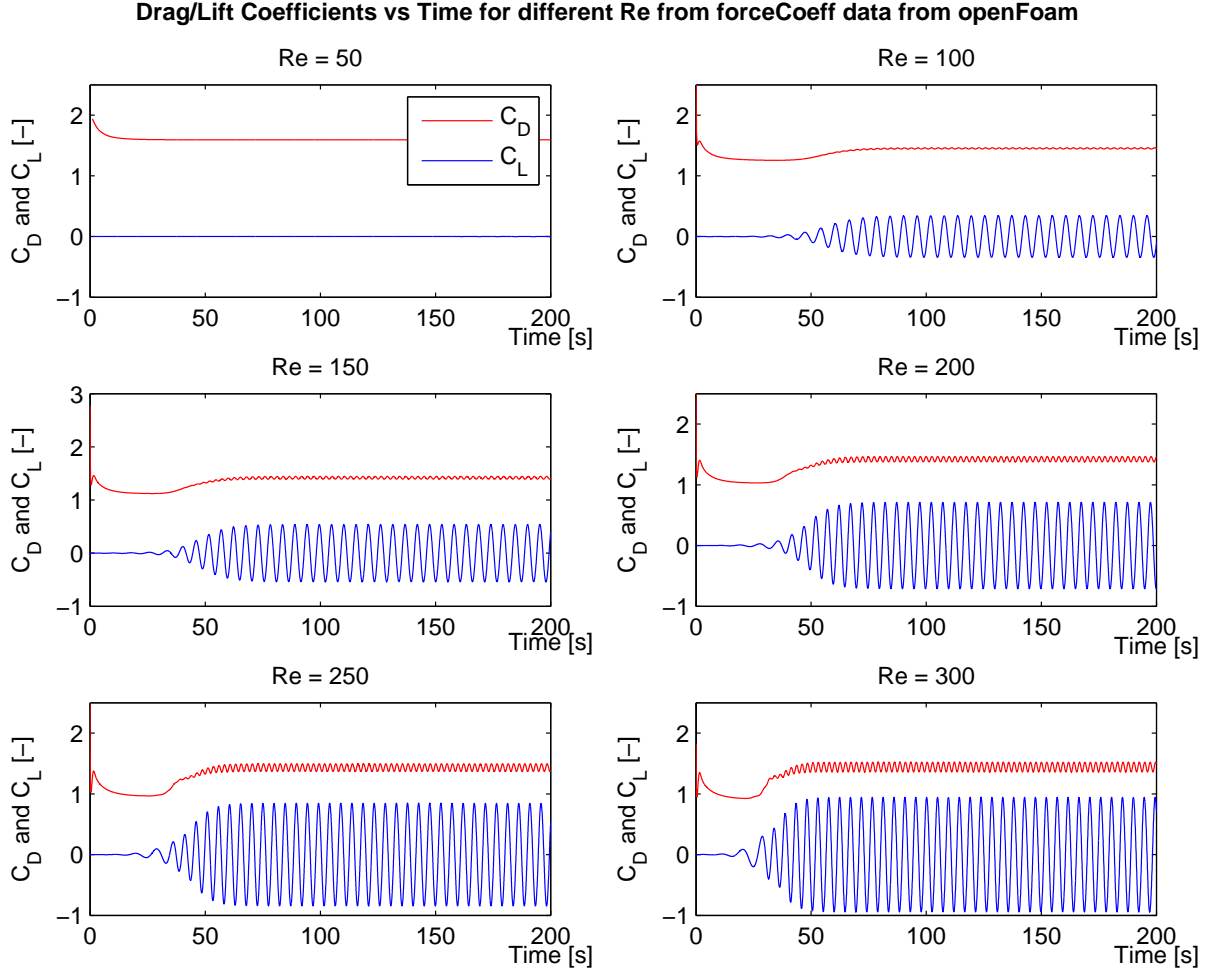
### forces/forceCoeffs utilities in openFoam

In openFoam, the user can calculate the induced drag/lift forces and drag/lift coefficients on objects by adding some commands in *system/controlDict* in the openFoam case file. Take a look in the `controlDict` file in the case folder to see an example of how to implement this. As a first test to see that the force/forceCoeffs are reliable, we now compare the data output of "forces" and "forceCoeffs" from openFoam. The data from "forces" are normalized according

to (5) with reference values  $A_{ref} = 1m^2$ ,  $U_\infty = 1m/s$ ,  $\rho = 1kg/m^3$ , such that the numeric difference between the two should only be a factor  $1/2$ . We plot the time series of the drag/lift forces and drag/lift coefficient and verify that their values are equal as seen in figure and figure. Note that the "forces" data has been multiplied by a factor 2 to produce the drag/lift coefficients according to (5).



**Figure 3:** Time series of  $C_D$  and  $C_L$  of simulations for  $Re = [50, 100, 150, 200, 250, 300]$  for a time span of  $t = [0, 200]s$ . The data is produced by taking the raw data from "forces" output from openFoam and thereafter computing  $C_D$  and  $C_L$  by computing  $C_D$  and  $C_L$  according to (5) with simulation reference values  $A_{ref} = 1m^2$ ,  $U_\infty = 1m/s$  and  $\rho = 1kg/m^3$ .

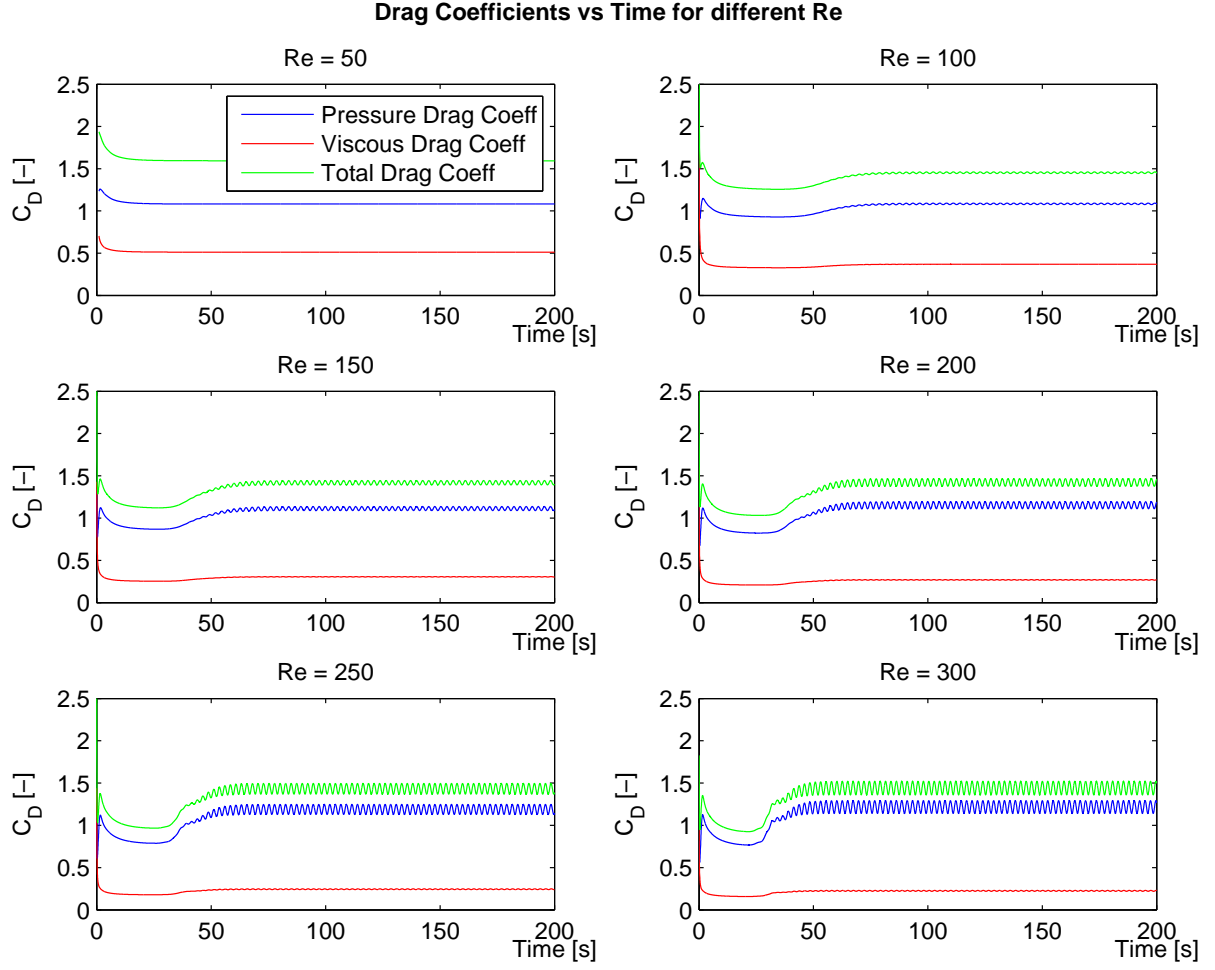


**Figure 4:** Time series of  $C_D$  and  $C_L$  of simulations for  $Re = [50, 100, 150, 200, 250, 300]$  for a time span of  $t = [0, 200]$ s. The data is the raw data produced by the "forceCoeffs" utility in openFoam.

Comparing figures 3 and 4 we can qualitatively verify that the data from "forces" and "forceCoeffs" is equal and that is all we wanted to show. This verifies that the data produces by "forces" and "forceCoeffs" in openFoam are indeed the same data in the sense that they differ only by the factors according to (5).

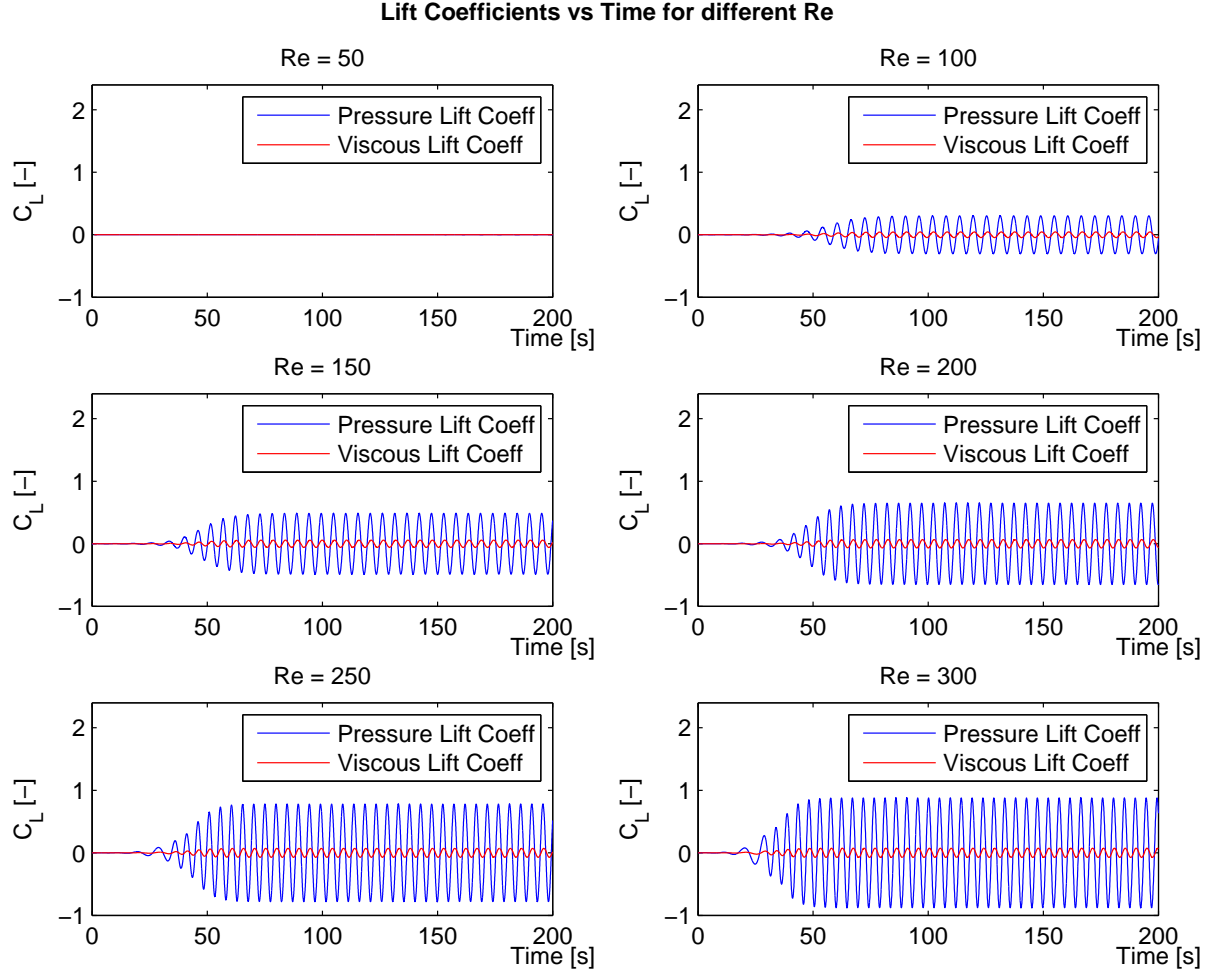
### Drag/Lift Forces for $50 < Re < 300$

Let us now look at the drag forces (forces acting in the x-direction) induced by the flow over the cylinder for various  $Re$ . In our case we have  $D = b = 1m$ , where  $b$  is the length in the z-direction, so  $A_{pro} = 1m^2$ . Furthermore we have set  $\rho = 1kg/m^3$  is the calculations to make it easy for ourselves. The following figure shows the drag force acting on the cylinder for various Reynolds numbers.



**Figure 5:** Drag Coefficient due to Pressure drag and Viscous drag for Reynolds numbers  $50 \leq Re \leq 300$ , with reference values  $\rho = 1 \text{ kg/m}^3$ ,  $A_{pro} = 1 \text{ m}^2$ ,  $U_\infty = 1 \text{ m/s}$ .

Figure 5 shows the drag coefficients due to pressure stress, viscous shear stress and total stress computed by openFoam. The drag coefficient are computed with reference values  $\rho = 1 \text{ kg/m}^3$ ,  $A_{pro} = 1 \text{ m}^2$  and  $U_\infty = 1 \text{ m/s}$ , and then the drag coefficients are computed according to (5). In the particular case of the above mentioned reference values, the drag force has half the numeric value as the drag coefficients. We see the pressure drag account for almost all the drag force, and the viscous drag is about an order of magnitude lower, as is expected for blunt bodies such as a cylinder. Secondly we see that the magnitude of the amplitude of the drag coefficient increases with Reynolds number. We also see that the force oscillations due to vortex shedding is too low to be captured in the case for  $Re = 50$ . We now turn our attention to the lift forces acting on the cylinder for various Reynolds numbers as seen in the following figure.

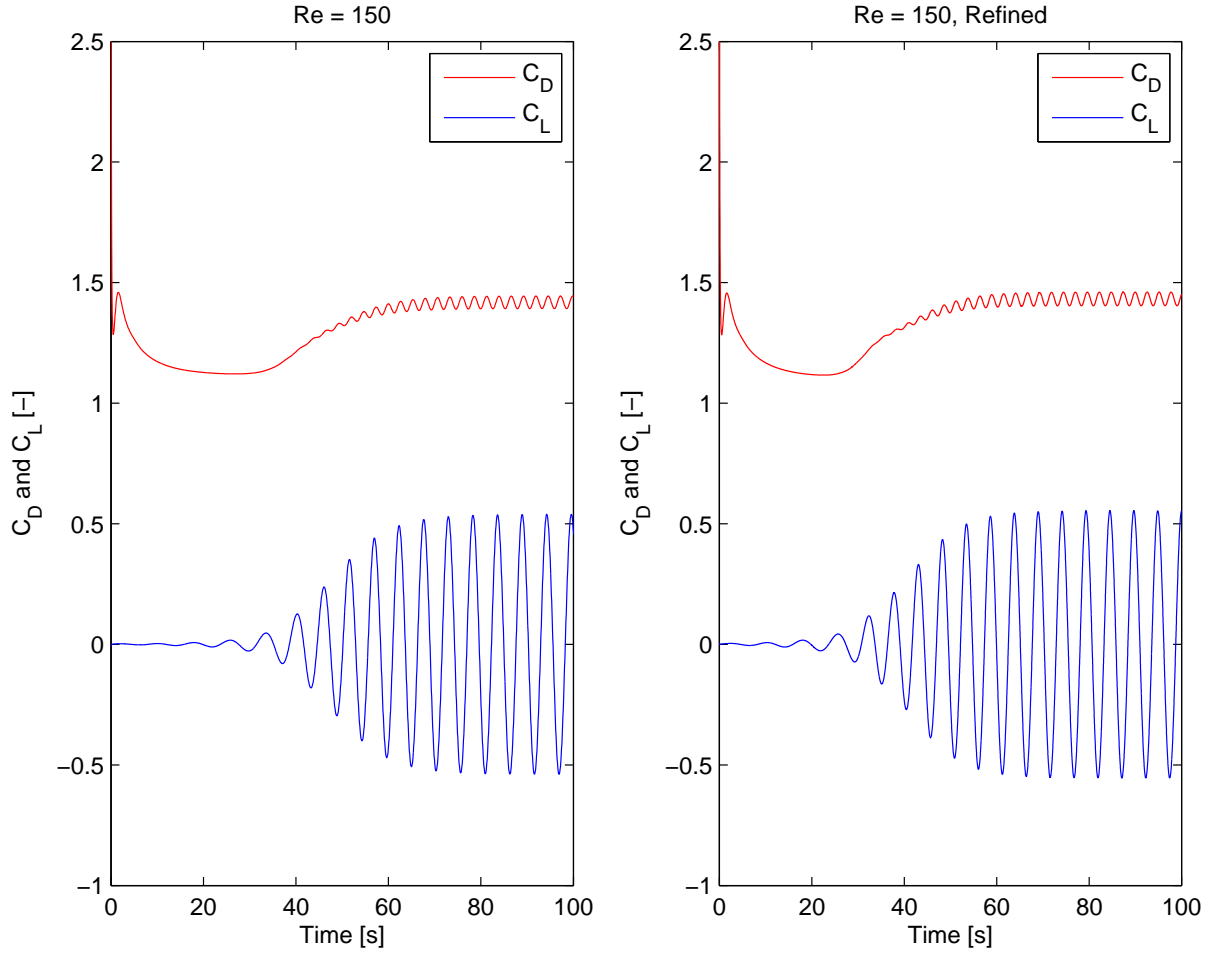


**Figure 6:** Lift Coefficients due to Pressure drag and Viscous stress for Reynolds numbers  $50 \leq Re \leq 300$ , with reference values  $\rho = 1\text{kg/m}^3$ ,  $A_{pro} = 1\text{m}^2$ ,  $U_\infty = 1\text{m/s}$ .

Figure 6 shows the lift coefficients due to pressure and viscous shear stress computed by openFoam. The lift coefficients are computed with the same reference values as above. We see that the lift force due to vortex shedding is mainly due to pressure oscillation, and that viscous lift oscillations are almost negligible.

### Comparison against a Mesh Refinement solution

The concept of *mesh independence* is very important in CFD. This states that the CFD solution should converge to a true solution as the grid is refined. At some threshold the solution does not change any more with increasingly refined grid. At this point we say that we have reached a mesh independent solution. Needless to say, this analysis can be very computationally expensive but nonetheless this analysis should be performed to make sure your simulation behaves as expected. In this tutorial we have performed one mesh refinement for  $Re = 150$ , and plotted the computed drag force time series as seen in the following figure.



**Figure 7:** Comparison of the drag and lift coefficient between the unrefined and refined mesh. The refined mesh has a twice the number of cells in the both the  $x$  and  $y$  direction compared to the unrefined mesh, thus it has a total of 4 times the number of cells compared to the unrefined mesh.

In figure 7 we see a comparison of the values of  $C_D$  and  $C_L$  between the unrefined and refined mesh. The refined mesh has twice the cell count in both  $x$  and  $y$  direction and thus has a total of 4 times the number of cells as the unrefined mesh. We see that qualitatively the values of  $C_D$  and  $C_L$  does not change between the two simulation, and this provides some evidence that the values are trustworthy. Note that this does not necessary mean that the solution is mesh independent. To show this we should ideally have compared the solutions produced by increasingly refined mesh against an analytical solution or other *very* trustworthy solution and seen that the deviation between the numerical and trustworthy solution fade off at a rate proportional to the truncation error of the numerical discretization schemes.

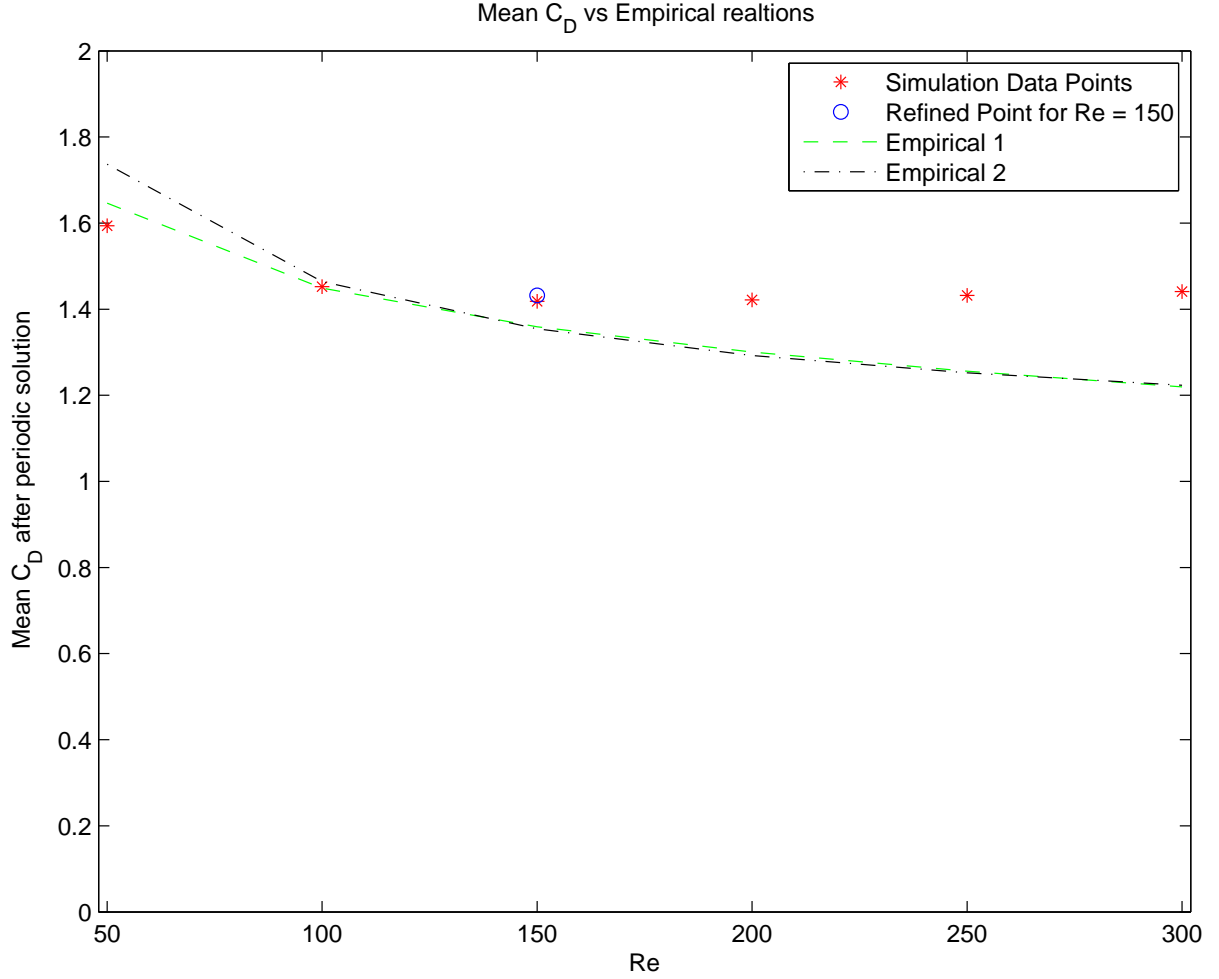
## Comparison against Empirical Relations

There is a number of empirical relations in the literature for drag coefficients over various bodies, two of which is given in [White] for flow across a cylinder.

$$C_D = 1.18 + \frac{6.8}{Re^{0.89}} + \frac{1.96}{Re^{\frac{1}{2}}} - \frac{0.0004Re}{1 + 3.64 \cdot 10^{-7} Re^2}, \quad 10^{-4} \leq Re \leq 2 \cdot 10^5 \quad (6)$$

$$C_D = 1 + \frac{10.0}{Re^{\frac{2}{3}}}, \quad Re \leq 2.5 \cdot 10^5 \quad (7)$$

A comparison of the of the computed drag coefficients with the empirical relations is shown in the following figure



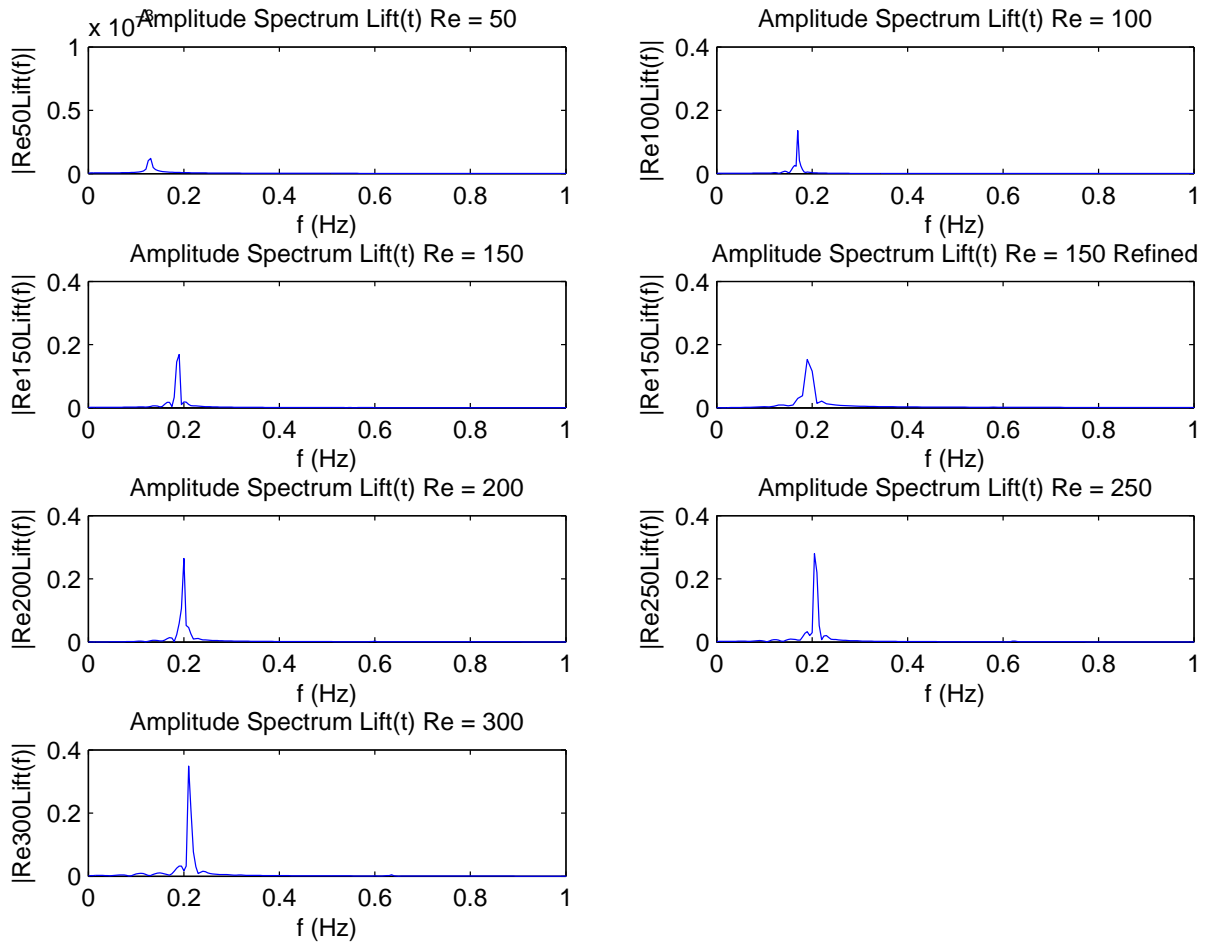
**Figure 8:** Mean drag coefficients compared with empirical relations for Reynolds numbers  $50 \leq Re \leq 300$ . Empirical 1 corresponds to (6), and Empirical 2 corresponds to (7). The mean values are computed from the time signals after the time signals has settled to a quasi steady state of pure oscillatory behaviour.

From figure 8 we see that the computed values tend to somewhat overestimate the empirical relations for our simulations in the range  $Re \in [50, 300]$ . In addition we see that the numerical results settle at a fairly constant value of  $C_D \approx 1.43$  where as the empirical has a slow decline in value, such that there is quite a significant deviance for  $Re = 300$ . There is a number of possible explanations of this. For one we know that transition to turbulence happens behind the wake within  $Re = [200, 300]$  and even though the boundary layer close to the cylinder wall still is laminar at  $Re = 300$ , it may still be possible that a possible turbulent wake may have

some influence on the computed drag coefficient. Secondly the empirical relations are designed to be valid over quite a large interval up to  $Re = 2.5 \times 10^5$  and therefore is mainly designed to capture the effects after turbulence kicks in after  $Re \approx 300$ . It may therefore be argued that the empirical relation is simply not designed very well to capture the drag coefficient for laminar flow, but this ought to be investigated further.

## Frequency analysis of Vortex Shedding

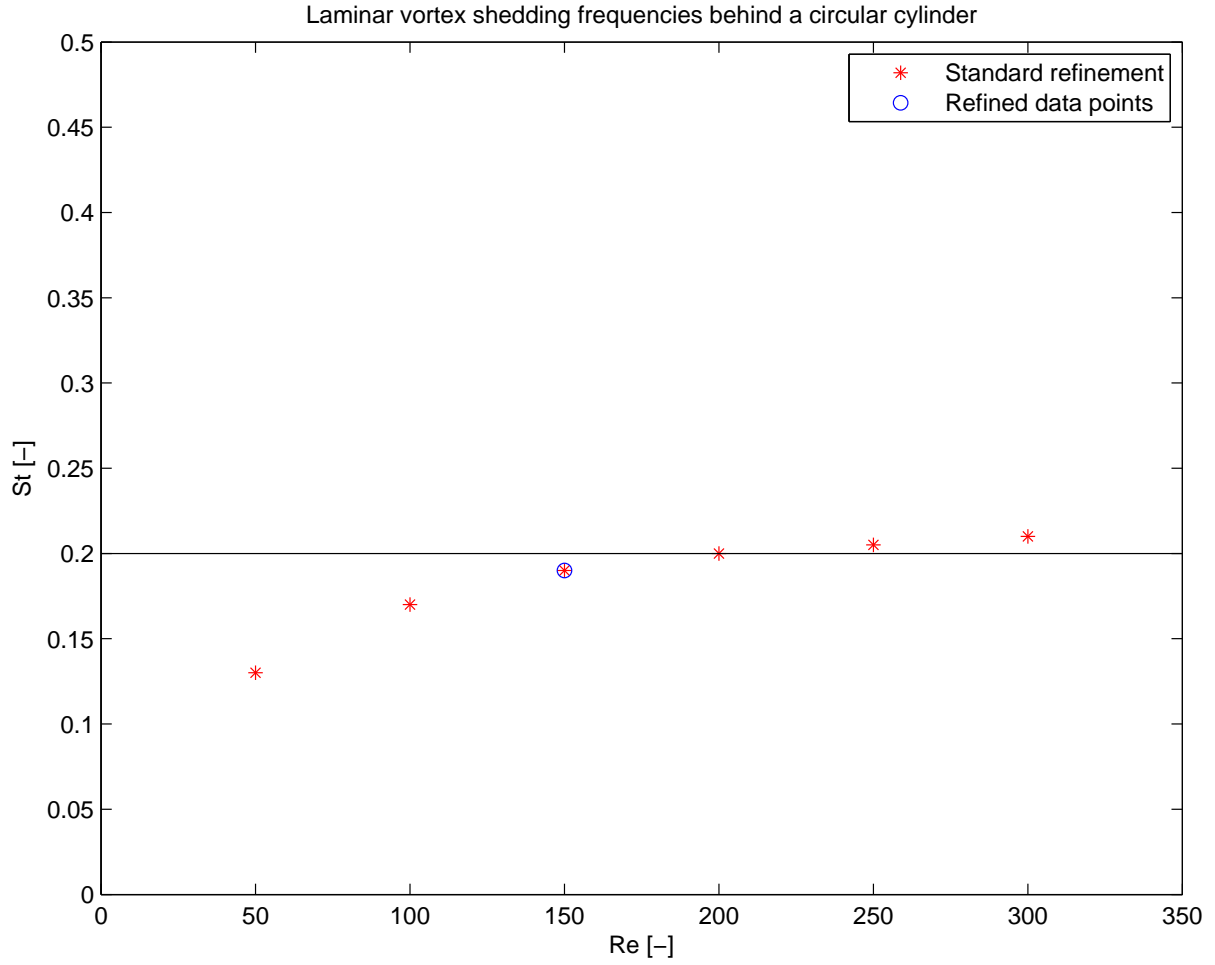
We close off this report by considering the functional relationship  $St = f(Re)$  as was developed in (2). We take the Fourier transform of the quasi steady time signals for the 6 different Reynold numbers with the FFT algorithm in Matlab as seen in the following figure.



**Figure 9:** Single sided amplitude spectrum of Fourier transform of the quasi steady (oscillatory) time signal.

Figure 9 shows the amplitude spectrum for the different Reynolds numbers. From this plot we can determine the frequency of the vortex shedding, and plot that frequency as a function of Reynolds number as seen in the following figure





**Figure 10:** Non dimensional frequency  $St$  as a function of  $Re$ .

As seen in figure 10 we see the non dimensional frequency  $St$  increases with  $Re$  and approaches a value of  $St \approx 0.2$ . This author has not found any empirical formulae to compare this value with, but this behaviour is in good qualitative accordance with available plots in the literature i.e. [White] *pg.11* which shows that  $St$  should increase gradually with  $Re$  and settle around a value of  $St \approx 0.2$ .

## Conclusions

This concludes this report on Laminar Vortex Shedding across a 2D Cylinder. We have performed simulations for Reynolds numbers  $Re = [50, 100, 150, 200, 250, 300]$  in openFoam. We have computed the drag and lift forces and coefficients with the "forces" and "forceCoeffs" post processing utility in openFoam and seen that despite the results are fairly reasonable, they tend to overestimate the value of the drag forces compared to empirical relations. Furthermore we have taken the Fourier transform of the time signals of the lift forces and plotted the functional relationship  $St = f(Re)$  and seen that the shedding frequency with Reynolds numbers and settle around a value of  $St = 0.2$  which is in good accordance with literature.

# Bibliography

- [Sumer et al] B. Mutlu Sumer, Jorgen Fredsoe  
*Hydrodynamics Around Cylindrical Structures*. World Scientific
- [White] Frank M. White  
*Viscous Fluid Flow*. McGraw-Hill 2006
- [Bakker] Andre Bakker  
*Lecture 7 Meshing*.